





PAPER

[View Article Online](#)
[View Journal](#) | [View Issue](#)Cite this: *Catal. Sci. Technol.*, 2019, 9, 4552

A step forward in solvent knitting strategies: ruthenium and gold phosphine complex polymerization results in effective heterogenized catalysts†

Antonio Valverde-González,  Gwendoline Marchal, 
Eva M. Maya * and Marta Iglesias *

Porous polymers based on ruthenium and gold triphenylphosphine complexes (KPhos(Ru), KPhos(Ru)Bi, KPhos(AuCl) and KPhos(AuNTf₂)) were prepared *via* a cost-effective solvent knitting method with [RuHClCO(PPh₃)₃] or AuXPPPh₃ (X = Cl, NTf₂) as single monomers or combined with biphenyl, which represents a further approach to obtain heterogenized catalysts. The resulting materials mainly preserve the metal coordination environment of their parent complexes, are stable up to 350 °C and have reasonable surface areas (250–300 m² g^{−1} for KPhos(Ru)-polymers). KPhos(Ru)s selectively catalyze the imination of alcohols in the presence of base and the results for KPhos(Au)s show they are effective for the intermolecular hydration and hydroamination of alkynes. These materials can be reused several times without significant loss of activity. This novel and simple method affords heterogenized catalysts that combine the reactivity and selectivity of their homogeneous counterparts with the stability and reusability of a heterogeneous framework.

Received 25th April 2019,
Accepted 12th July 2019

DOI: 10.1039/c9cy00776h

rsc.li/catalysis

Introduction

Heterogenized catalysts are usually prepared by immobilizing a homogeneous catalyst onto a solid support and have shown significant benefits in stability, recyclability over multiple cycles, and separation from the reactants.¹ Silica-based materials² and magnetic nanoparticles³ are usually used as supports, but they have the disadvantages of a lack of homogeneity of the active sites and eventual blocking of the pores and deactivation of the catalyst.⁴ Over the last few years porous hybrid organo–inorganic materials (MOFs),⁵ and porous organic materials as porous organic polymers (POPs)⁶ or covalent organic frameworks (COFs)⁷ have been used as solid porous platforms to heterogenize homogeneous catalysts. In general, POPs show high hydrothermal and chemical stability and could be converted into catalysts by incorporation of catalytic sites as building blocks by covalent bonds and can be modified by post-synthetic methods.⁸

Hyper-cross-linked polymers synthesized by a knitting polymerization method (employing AlCl₃ or FeCl₃ as a cata-

lyst and dichloromethane or dimethoxymethane as a cross-linker)⁹ are a relative new family of porous polymers with excellent properties, such as high thermal and chemical stability, insolubility and easy post-functionalization for use as supports for homogeneous catalysts. This method has been applied to prepare several series of porous polymers from different aromatic monomers.^{6f,10}

Nonetheless, the maintenance of the coordination metal environment through this strategy has not always been pursued. Lai and co-workers reported the direct knitting of palladium tetrakis(triphenylphosphine) and benzene where the palladium atoms were spatially isolated in the framework of the polymer.¹¹ Alternatively, Song and co-workers knitted 1,1'-bis(diphenylphosphino)ferrocene and biphenyl, affording an effective catalyst for the reduction of 4-nitrophenol, where the ferrocenyl units were not altered.¹² Recently, during the preparation of this manuscript, Huang's group achieved a highly effective catalyst for the dehydrogenation of formic acid to hydrogen by knitting a pincer ruthenium complex and benzene.¹³

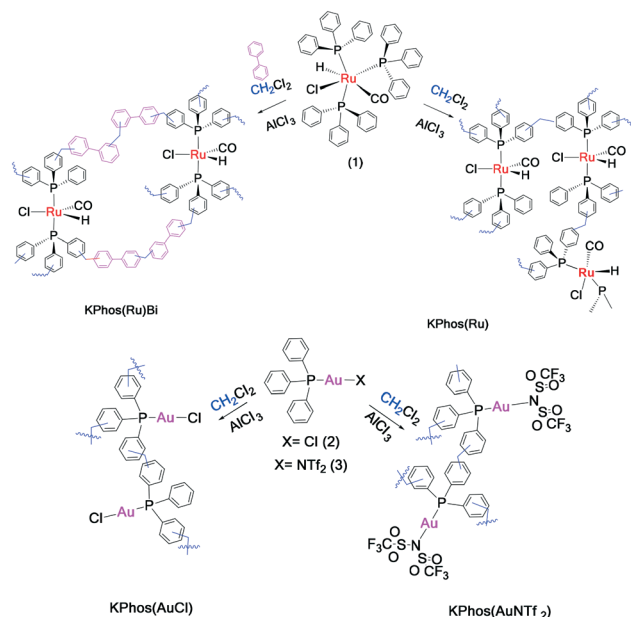
Here, we present an easy synthesis of new knitted metal-based polymers that maintains the molecular structure of the parent Ru- and Au-complexes (Scheme 1); these materials result in effective heterogenized metal-triphenylphosphine catalysts for the synthesis of imines, in the case of the Ru-based polymers, and for the hydration of alkynes, in the case of the Au-based catalysts.

Instituto de Ciencia de Materiales de Madrid, CSIC, c/Sor Juana Inés de la Cruz 3, Cantoblanco, Madrid 28049, Spain. E-mail: marta.iglesias@icmm.csic.es

† Electronic supplementary information (ESI) available. See DOI: 10.1039/c9cy00776h

‡ Present address: Ecole Nationale Supérieure de Chimie de Mulhouse, 3 rue Alfred Werner 68093, Mulhouse, Cedex, France.





Scheme 1 Synthesis of knitted ruthenium and gold-phosphine-polymers.

Results and discussion

The knitted ruthenium and gold-phosphine-polymers (**KPhos(Ru)**, **KPhos(Ru)Bi**, **KPhos(AuCl)**, **KPhos(AuNTf₂)**) were synthesized in a one-step hyper-crosslinking method *via* an AlCl_3 -catalyzed reaction (Scheme 1).¹⁰ In this method, dichloromethane was employed as an external methylene linker between the phenyl groups from the phosphine ligands in the parent ruthenium $[\text{RuHClCO}(\text{PPh}_3)_3]$ or AuXPPH_3 ($\text{X} = \text{Cl}$, NTf_2) complexes. In the case of **KPhos(Ru)Bi**, the polymerization occurs in the presence of biphenyl, which acts as a co-monomer in a molar ratio of 2:1 *versus* the ruthenium complex.

The resulting polymers are insoluble in water, alcohol or the most common organic solvents. The formation of the hyper-cross-linked metal-phosphine complex network is confirmed by FTIR, solid-state ^{13}C -NMR, ^{31}P -NMR, thermal analysis (TGA), and SEM and TEM microscopies. X-ray photoelectron spectroscopy (XPS) confirms the oxidation state of ruthenium, gold and phosphorous. The metal loading was determined by transmission X-ray fluorescence spectroscopy (TXRF) or ICP-OES¹⁴ with the results: 2.26 mmol g^{-1} , 22% weight (**KPhos(Ru)**), 0.79 mmol g^{-1} , 8% weight (**KPhos(Ru)Bi**), 0.72 mmol g^{-1} , 15% weight (**KPhos(AuNTf₂)**) and 0.97 mmol g^{-1} , 19% weight (**KPhos(AuCl)**). SEM-EDX analyses confirmed that the ratios of P:Ru and P:Au are 2:1 and 1:1, respectively (Fig. S17†). These results are in good agreement with the inorganic residue obtained by TGA.

The ^{13}C -CP/MAS-NMR spectra of the polymers (Fig. 1) displayed a peak at $\delta = 41.2 \text{ ppm}$ corresponding to methylene linker, from CH_2Cl_2 , which confirms the successful C-C coupling.¹⁵ The CO signals could not be identified because of the low sensitivity of solid-state NMR spectroscopy. The peaks

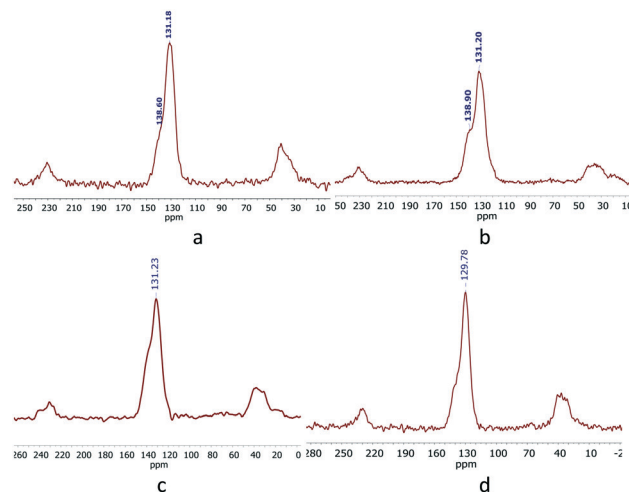


Fig. 1 ^{13}C -NMR spectra of a) **KPhos(Ru)**, b) **KPhos(Ru)Bi**, c) **KPhos(AuCl)** and d) **KPhos(AuNTf₂)**.

at $\delta \sim 139$ (sh) and 131 ppm correspond to aromatic carbons from triphenylphosphine ligands.¹⁶ The ^{31}P -MAS-NMR spectra (Fig. S1 and S2†) show peaks at 28 and 26 ppm for both **KPhos(Ru)** and **KPhos(Ru)Bi** polymers, at 29 ppm for **KPhos(AuCl)** and at 26 ppm for **KPhos(AuNTf₂)** which confirm the presence of P-Ru and P-Au bonds. Further peaks at $\delta \sim 60$ –70 ppm are attributable to phosphorous species generated by the polymerization process (for example ionic phosphonium species such as $(\text{PPh}_3\text{Cl})\text{Cl}$).¹⁷ It is important to note that no free phosphine (at $\sim 5 \text{ ppm}$) was observed.

FTIR spectra (Fig. 2) show bands at 2058 and 1980 cm^{-1} corresponding to $\nu(\text{Ru-H})$ and $\nu(\text{CO})$, respectively, confirming that the molecular structure is mainly maintained after the polymerization process; some other vibration bands are also present, such as $\nu(\text{C-H})$ at 3100 cm^{-1} , $\nu(\text{C-C})$ at $\sim 1400 \text{ cm}^{-1}$ from triphenylphosphine moieties and $\nu(\text{P-C})$ at 1100 cm^{-1} . The **KPhos(Ru)Bi** spectrum also shows an extra band at $\sim 1600 \text{ cm}^{-1}$ corresponding to the $\text{C}=\text{C}$ vibration from

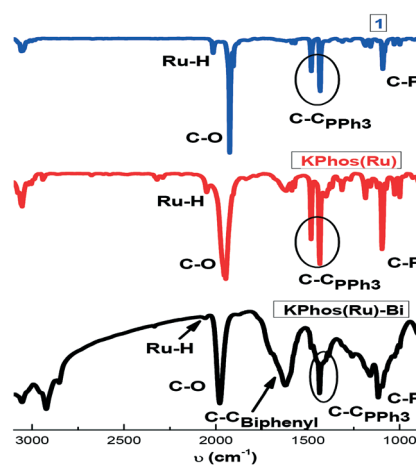


Fig. 2 FTIR spectra of the parent Ru-complex and knitted $\text{Ru}(\text{PPh}_3)$ -polymers.



biphenyl. The FT-IR spectra of the gold-polymers are shown in Fig. S5†

Fig. S16† shows the XPS survey scans of the polymers. Ru was analysed by its 3p state instead of the 3d spectra to avoid the overlap of the C1s and Ru3d core-levels. The Ru3p region (Fig. 3a) shows a doublet peak at 464 eV and 485 eV for Ru3p_{3/2} and Ru3p_{1/2}, respectively, for the RuP species, which confirms that ruthenium has the +2-oxidation state.¹⁸ The P2p spectrum (Fig. 3b) showed the presence of only one P-containing species at 133.0 eV, assigned to the PPh₃ species. For KPhos(AuCl), the binding energy of Au4f at 86 eV justifies the presence of the gold(I) oxidation state (Fig. 3c); the typical P2p binding energy was observed at 134 eV, confirming that no triphenylphosphine oxide was present in the sample. These results confirm that the oxidation state of the polymer is preserved.

Thermogravimetric analyses (TGA) (Fig. 4) showed a one-step degradation pattern for all the knitted metal-phosphine polymers. KPhos(Ru)Bi exhibited higher thermal stability than KPhos(Ru) with thermal decomposition temperatures of 380 °C and 300 °C, respectively. Whereas knitted gold-phosphine polymers showed similar degradation temperatures around 350 °C. As commented previously, the metal content was confirmed by TGA. At high temperatures, gold, ruthenium and phosphine oxides are formed, Au₂O₃, RuO₂ and P₂O₅; however, at 200 °C Au₂O₃ decomposed into Au and O₂.¹⁹ Therefore, considering that the Ru-polymer residue is RuO₂ and P₂O₅ and Au and P₂O₅ for the Au-polymers, it was possible to estimate the gold, ruthenium and phosphorous loading by TGA analyses which were in good agreement with those obtained by TXRF and ICP-OES, as given above.

The N₂ adsorption isotherms of both KPhos(Ru)Bi and KPhos(Ru) displayed the same type II profile. The Brunauer–Emmett–Teller (BET) surface areas were 250 m² g⁻¹ and 300 m² g⁻¹ (Fig. 5, Table 1) and the total pore volumes were found

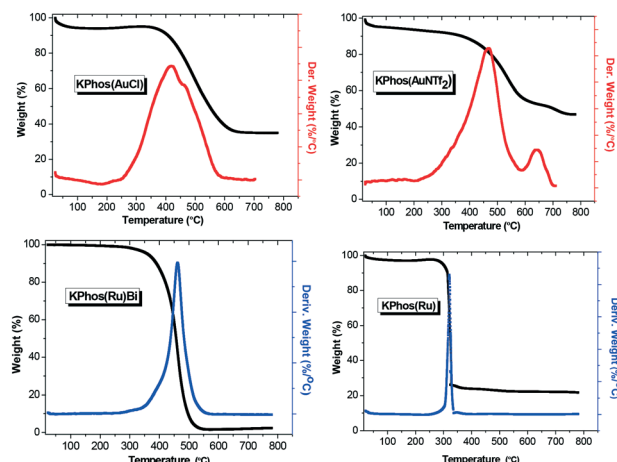


Fig. 4 Thermal analysis of KPhos(AuX) (top) and KPhos(Ru) (bottom).

to be 0.11 and 0.20 cm³ g⁻¹, respectively. The pore distributions were calculated by the N₂-DFT method (Fig. S13†). The plot shows that pore sizes were mainly distributed around 2.4 nm, indicating that mesopores were present in both polymers. Furthermore KPhos(Ru)Bi also exhibited mesopores around 40 nm. KPhos(AuNTf₂) and KPhos(AuCl) polymers showed low N₂ adsorption (Fig. S14, A and B†) affording only 20 and 49 m² g⁻¹ of specific surface areas, respectively.

The surface morphology was explored by field-emission scanning electron microscopy (SEM) and transmission electron microscopy (TEM) (Fig. 6 and S7–S12†) showing the typical morphology described for this type of porous organic polymer, made up of aggregates of spherical structures that resemble the texture of a sponge. In addition, energy-dispersive X-ray spectroscopy (SEM–EDX) and elemental mapping analysis revealed coherent ratios of Ru/P and Au/P (see the ESI†, Fig. S17).

Post-functionalization of triphenylphosphine knitted polymers (KPhosBi(M), M: Ru, Au)

For comparative purposes, we have tried to prepare polymers following a post-functionalization strategy (Scheme 2), using

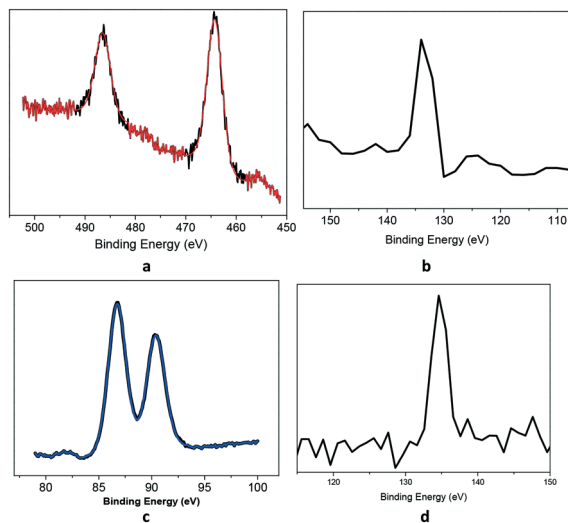


Fig. 3 Core-level XPS spectra: (a) Ru(3p) and (b) P(2p) (KPhos(Ru)) (top), and (c) Au(4f) and (d) P(2p) (KPhos(AuCl)) (bottom).

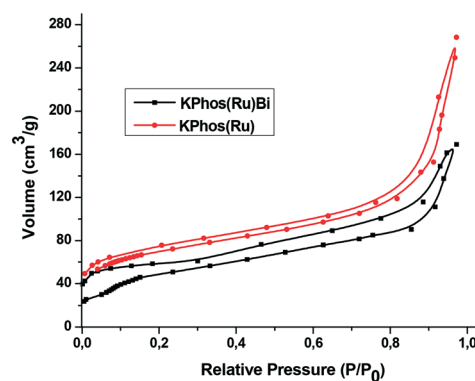
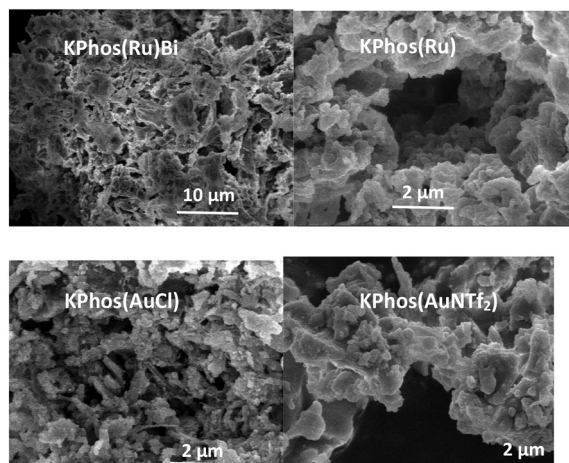


Fig. 5 Nitrogen adsorption/desorption isotherms of KPhos(Ru) polymers.



Table 1 Physical properties of KPhos-polymers

Polymer	S_{BET} ($\text{m}^2 \text{g}^{-1}$)	V_{TOTAL}^a ($\text{cm}^3 \text{g}^{-1}$)	D_{pore} (nm)
KPhos(Ru)	300	0.203	2.2
KPhos(Ru)Bi	250	0.107	2.2
KPhosBi	704	1.45	8.3
KPhos(AuNTf ₂)	20	0.12	1.7
KPhos(AuCl)	49	0.07	5.9

^a At $P/P_0 = 0.99$.**Fig. 6** SEM images of KPhos polymers.

a similar approach to that previously reported with benzene as a co-linker.²⁰ Triphenylphosphine was reacted with biphenyl (molar ratio 1 : 1) in the presence of AlCl_3 and dimethoxy-methane as an external linker in dichloroethane (DCE) as a solvent, yielding a polymer denoted **KPhosBi**. It showed a BET surface area of $704 \text{ m}^2 \text{g}^{-1}$ (Table 1) (N_2 adsorption/desorption isotherm, Fig. S15[†]). Its NMR solid state spectra are shown in Fig. S3[†]. Then, **KPhosBi** was reacted with $\text{RuCl}_3 \cdot \text{nH}_2\text{O}$, following a similar method to the one used to synthe-

size the precursor $\text{RuHClCO}(\text{PPh}_3)_3$. However, TXRF and XPS analyses of the resulting solid revealed that the ruthenium loading in **KPhosBi(Ru)** is only 0.02 mmol g^{-1} (Fig. S16[†]). Therefore, we discarded this approach to heterogenizing the Ru-phosphine complex. Alternatively, **KPhosBi** was reacted with $\text{AuCl}(\text{tht})$ in dichloromethane, affording the corresponding **KPhosBi(Au)** polymer. ICP-OES analysis revealed that the gold loading was 1.01 mmol g^{-1} . The ^{31}P -NMR spectrum shows that P-Au and phosphine moieties are present in the polymer (Fig. S4[†]). XPS analysis shows a doublet corresponding to Au4f at around 85 eV. In both spectra, the characteristic phosphine peak of P2p was observed at around 136 eV (Fig. S16[†]). In this case, it seems that the corresponding supported Au-phosphine complex has been formed.

Catalytic applications

KPhos(Ru): imination of alcohols. This reaction, from unreactive alcohols without an oxidant, is an important non-polluting route to provide aldehydes and related products.²¹ On the other hand, imines are important compounds in modern organic synthesis because they are key intermediates in the synthesis of nitrogen-containing heterocycles.²² Generally, imines are formed by condensation of ketones or aldehydes and amines, catalysed by an acid. Due to the instability of the carbonyl group, the synthesis of imines from more stable and low-cost reactants, such as alcohols, has attracted considerable attention, with the aerobic oxidative coupling of alcohols and amines the most promising strategy.²³

It is well known that ruthenium is a widely used and versatile catalyst for the dehydrogenation of alcohols.²⁴ However, it is hardly used for the imination reaction.²⁵ Ru-parent complex **1** is an efficient homogeneous catalyst in reactions such as the hydrogenation of aldehydes and ketones, transfer hydrogenation or transfer hydrogenative C-C bond forming reactions.²⁶ Thus, these data prompted us to study a possible imination reaction from alcohols and amines with knitted Ru-polymers as heterogeneous catalysts and the results were compared with those obtained from a homogeneous **1**-complex. Since **KPhos(Ru)** and **KPhos(Ru)Bi** have similar characteristics, we chose **KPhos(Ru)** as the reference catalyst. Reaction of 1.2 mmol of benzyl alcohol, 1.0 mmol of aniline and 2 mol% of catalyst in toluene at 100°C for 2 h in the presence of a base, quantitatively afforded *N*-benzylidenebenzylamine (96% selectivity) (Table 2, entry 1). Previous experiments revealed that the reaction in the presence of KOH resulted in longer reaction times (entry 4) than using potassium *tert*-butoxide (entry 3), to achieve a similar conversion with the same substrate. Moreover, it was tested that the reaction did not occur without a base (entry 5). The reaction was not efficient at room temperature and the best results were obtained in toluene at 100°C . In the absence of a catalyst, only traces of product were obtained (entry 6).

The substrate scope was examined under optimized conditions. Electron-rich 4-methoxyaniline, benzylamine and 1-octylamine gave excellent conversions and selectivity into

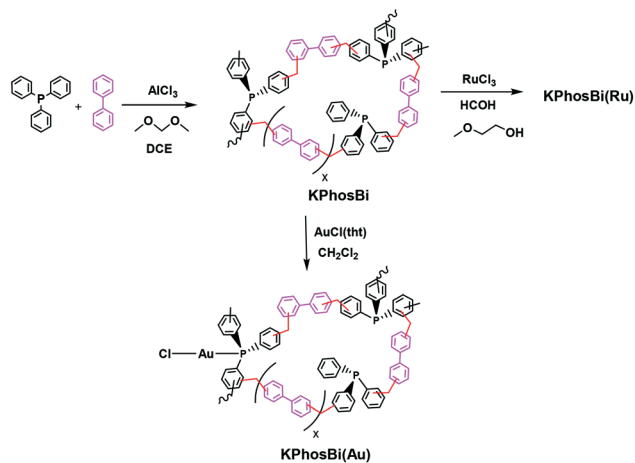
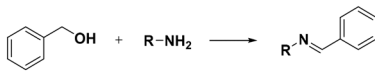
**Scheme 2** Synthetic route for post-functionalized **KPhosBi(M)** polymers.

Table 2 Imination of benzyl alcohol with aryl amines catalyzed by **KPhos(Ru)**^a

						
Entry	Catalyst	Base	R	<i>t</i> (h)	Conv. (%)	Sel. (%)
1	KPhos(Ru)	KO ^t Bu	Ph	2	100	96
2	RuHCl(CO)(PPh₃)₃ ^b	KO ^t Bu	Ph	0.5	100	98
3	KPhos(Ru)	KO ^t Bu	4-OMe-Ph	1.5	100	100
4	KPhos(Ru)	KOH	4-OMe-Ph	4	97	100
5	KPhos(Ru)	None	Ph	20	0	—
6	None	KO ^t Bu	Ph	6	0.8	100
7	KPhos(Ru)	KO ^t Bu	PhCH ₂	2	100	100
8	KPhos(Ru)	KO ^t Bu	CH ₃ (CH ₂) ₇	4	100	100
9	KPhos(Ru)	KO ^t Bu	4-Br-Ph	20	90	100

^a Reaction conditions: *T*: 100 °C, amine (1.0 mmol), benzyl alcohol (1.2 mmol), toluene (0.5 mL), base (0.05 mol%), cat. (2.0% mmol based on Ru). ^b 0.5% mol.

the corresponding imines (Table 2, entries 3, 7, 8), and 4-bromoaniline afforded 90% conversion after 20 h of reaction (entry 9).

The possibility of recycling and reusing the catalyst, along with the occurrence of leaching processes, were examined under the conditions in entry 1. Recycling experiments show that the activity of **KPhos(Ru)** does partially decrease after two cycles, probably due to some loss of catalyst during filtration, and more time is needed to achieve >90% conversion (Fig. 7). In order to evaluate whether the structure of the catalyst had changed after recycling, we undertook XPS analysis of the recovered catalyst (Fig. S21†). The XPS spectrum in the region of Ru3p and P2p is very similar to that of fresh Ru-polymer. FT-IR after recycling (see Fig. S6†) shows that $\nu(\text{Ru-H})$ appears as weak signal at 2055 cm⁻¹ and $\nu(\text{CO})$ at 1982 cm⁻¹ which indicates that the coordination environment of ruthenium in the polymer is mainly maintained. Gratifyingly, no leaching of active ruthenium species occurred. Upon removal of the catalyst by hot filtration after 30 minutes of reaction, the conversion remained unaltered for 3 h (Fig. S18b†).

KPhos(Ru) was also investigated for the transfer hydrogenation of acetophenone in *i*-PrOH at reflux, resulting in total conversion after 16 h of reaction. The reaction between ben-

zyl alcohol and acetophenone leads to a mixture of condensation products ketone/alcohol (80/20).

Based on our results and previous reports, the proposed mechanism for the alkylation of amine with alcohol²⁷ is that a Ru-alkoxide intermediate is formed under basic conditions, which catalyses the dehydrogenation of alcohol to a carbonyl compound, and subsequently, the base promotes the condensation of carbonyl compound with amine to imine.

KPhos(AuX): hydration of alkynes. Hydration of alkynes is a very environmentally benign method to form carbon-oxygen bonds. Furthermore, it has been extensively studied that the efficiency of this reaction lies in the coordination environment of the gold centre, being far more active when it forms a cation, although the nature of the corresponding contra-anion can also have an effect. The hydration of phenylacetylene was selected as a model reaction to test the catalytic activity of **KPhos(AuX)** (X = Cl, NTf₂) polymers in the presence of different co-catalysts.

First, we carried out reactions with **KPhos(AuCl)** polymer in the presence of different silver-containing cocatalysts (Table 3, entries 1–3) in order to remove the halide coordinated to the gold(i) centres and generate catalytically suitable species for substrate activation ([PPh₃Au]⁺ species). It was found that the best results were obtained in the presence of silver triflimide because the triflimide anion stabilizes the cation [PPh₃Au]⁺, and in all cases, the ketone was obtained. The reaction evolution in the presence of silver co-catalysts is shown in Fig. S19.† Therefore, the system **KPhos(AuCl)/AgNTf₂** was employed with different terminal alkynes affording total conversion after 1 h of reaction (entries 11–13). However, when the internal alkyne methylphenylacetylene was employed, the reaction did not occur even after 20 hours (entry 14).

Some other silver-free co-catalysts were used, such as: CH₃CN/NH₄BF₄, TfOH and LiNTf₂ (entries 4–6). Again, the best results were obtained in the presence of lithium triflimide (entry 6). However, longer reaction times were necessary to achieve 100% yield. Rather, when the post-functionalized **KPhosBi(AuCl)/LiNTf₂** system was applied as a

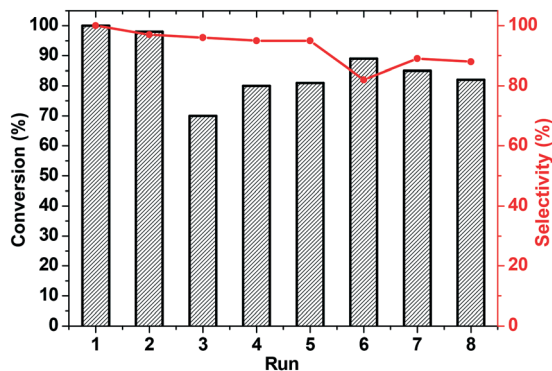
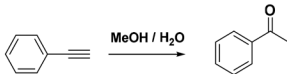
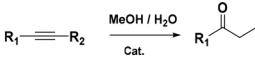

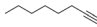
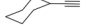
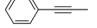
**Fig. 7** Recycling experiments with **KPhos(Ru)**, at 2 h reaction time.

Table 3 Catalyzed hydration of alkynes^a

			
Entry	Catalyst	<i>t</i> (h)	Yield (%)
1	KPhos(AuCl)/AgNTf ₂	1	100
2	KPhos(AuCl)/AgOTf	1.5	60
3	KPhos(AuCl)/AgBF ₄	10	40
4	KPhos(AuCl)/CH ₃ CN/NH ₄ BF ₄	2	25
5	KPhos(AuCl)/TfOH	3	20
6	KPhos(AuCl)/LiNTf ₂	3	100
7	KPhosBi(AuCl)/LiNTf ₂	20	80
8	KPhos(AuCl)/–	28	2
9	AuCl(PPh ₃)/AgBF ₄	10	45
10	AuCl(PPh ₃)/–	30	40

				
Entry	Catalyst	Alkyne	<i>t</i> (h)	Yield (%)
11	KPhos(AuCl)/AgNTf ₂		1	100
12			1	100
13			1	100
14			20	Traces

^a Reaction conditions: *T*: 60 °C, alkyne (0.2 mmol), MeOH (0.4 mL), H₂O (20 μL) cat 5 mol% (based on Au), co-catalyst: 5.5 mol%.

catalyst, only traces of hydrated product were detected after 3 hours of reaction, and longer reaction times were necessary to achieve good conversion (entry 7).

The use of silver salts as cocatalysts significantly affected the reusability of the catalyst, since after three cycles the catalyst lost its efficiency. This might be a consequence of the so-called ‘silver effect’, reported by Shi and coworkers,²⁸ which suggests that silver cations not only activate gold moieties but also modify them, affording different inactive complexes. Subsequently, the possibility of recycling the catalyst, along with the occurrence of leaching processes, was examined with the KPhos(AuCl)/LiNTf₂ system. Even though the catalyst life has been increased, it can clearly be observed that its activity decreases in each cycle (Fig. 8). Therefore, we tried to regenerate the catalyst by treating it with LiNTf₂ in methanol overnight, and we observed that the activity increased slightly up to 70%.

With the previous results in hand, we explored the catalytic activity of KPhos(AuNTf₂) under standard conditions (Table 4). It was found that 4-methoxy phenylacetylene and 1-octyne quantitatively yields the ketone after 1 h in the presence of 20 μL of water (entries 1 & 3); when the reaction was performed without water the ketone was not obtained (entries 2 & 4). When the same conditions were applied to internal alkynes, it was found that methyl phenylacetylene led selectively to the ketone after 3 h of reaction with a higher amount of water (entry 6); however, diphenylacetylene only yields the enol ether (Table 3, product A) after 22 h (entries 7, 8) and 1,4-dichlorobut-2-yne does not react (entry 9). These findings suggest the following: (A) the ketone is only formed

after hydration of ketal, as was previously reported by Corma *et al.*²⁹ (B) The ketal of the terminal alkyne undergoes hydration to ketone faster than those of the internal alkynes.

In order to verify the heterogeneity of the gold-catalyst, a hot filtration experiment was carried out. After 20 minutes, the solid was separated from the reaction media and the filtrate was stirred under the same conditions. Since the conversion did not increase after hot filtration, this experiment confirmed that no leaching occurs during the process (see Fig. S20†).

Finally, recycling of KPhos(AuNTf₂) using 4-methoxy phenylacetylene as a substrate was performed under entry 1 conditions. As can be observed in Fig. 9, the catalyst maintains its activity for ten cycles; however, the selectivity decreases after the third run and decreases to 40% in the sixth cycle. It is therefore necessary to regenerate the catalyst,

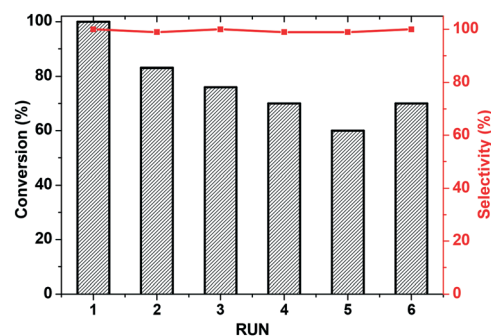


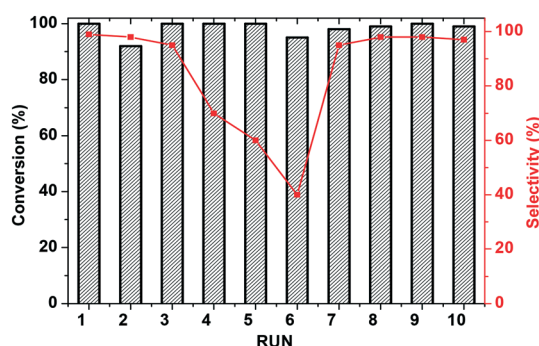
Fig. 8 Recycling experiments with the KPhos(AuCl)/LiNTf₂ catalytic system.



Table 4 Hydration of alkynes catalysed by $\text{KPhos}(\text{AuNTf}_2)^a$

$\text{R}_1\text{—}\text{C}\equiv\text{C—R}_2 \xrightarrow{\text{MeOH/H}_2\text{O}} \text{R}_1\text{—}\text{C}(\text{OCH}_3)=\text{C}(\text{R}_2)\text{—R}_1 + \text{R}_1\text{—}\text{C}(\text{OCH}_3)(\text{R}_2)\text{—C}(\text{OCH}_3)(\text{R}_2)\text{—R}_1 + \text{R}_1\text{—}\text{C}(=\text{O})\text{—R}_2$					
Entry	Alkyne	H_2O (μL)	t (h)	Conv. (%)	Selec. (%) (A/B/C)
1		20	1	100	0/0/100
2		—	2	80	90/10/0
3		20	1	100	0/traces/99
4		—	1	75	70/30/0
5		20	3	100	15/85/0
6		40	3	100	0/0/100
7		20	3	30	100/0/0
8		—	22	75	100/0/0
9		20	22	0	—

^a Reaction conditions: T : 60 °C, alkyne (0.2 mmol), MeOH (0.4 mL), cat (10 mg, 7.2 μmol , 2.8 mol% based on Au).

**Fig. 9** Recycling experiments with KPhosAuNTf_2 (1 h reaction time).

which is carried out by stirring it in methanol in the presence of LiNTf_2 overnight. This reactivation resulted in an increase in the selectivity to 100% for four more cycles.

KPhos(AuX): hydroamination of alkynes. The catalytic performance of the $\text{KPhos}(\text{Au})$ -complexes was also tested in the hydroamination of phenyl acetylene with aniline as a model reaction in the presence of a cocatalyst (silver salts or $\text{CH}_3\text{CN}/\text{NH}_4\text{BF}_4$).³⁰ Screening of cocatalysts was performed at 70 °C and, as can be seen in Table 5, the performance of $\text{KPhos}(\text{AuCl})$ depends on the silver salt anion. Anions of tetra-

fluoroborate were found to be detrimental to the process, whereas triflate enabled a much better performance and triflimide stood out as the best choice, as with the hydration of alkynes. It is important to note that when the reaction was carried out with $\text{KPhos}(\text{AuNTf}_2)$ (without any cocatalyst), the product was obtained selectively in 2 h with high yield (entry 1).

Conclusions

This manuscript presents four new heterogenized catalysts formed by the polymerization of phosphine metal complexes *via* a solvent knitting method. In this way, the polymerization of $\text{RuH}(\text{CO})\text{Cl}(\text{PPh}_3)_3$ resulted in a single-site robust material, which maintained its catalytic activity after six cycles in the synthesis of imines. On the other hand, the highly active homogeneous catalyst $\text{Au}(\text{PPh}_3)\text{NTf}_2$ was polymerized by the same procedure, leading to a heterogeneous framework that also maintained its catalytic activity even after 10 cycles in the hydration of alkynes and proved to be active in the hydroamination of alkynes.

In conclusion, we have extended a knitting polymerization strategy to the field of transition metal complexes, affording a straightforward route to obtain metal-containing polymers and opening up the possibility of heterogenizing many other soluble catalysts.

Table 5 Effect of the co-catalyst in the hydroamination of phenylacetylene with aniline promoted by $\text{KPhos}(\text{Au})$ -polymers^a

$\text{Ph—C}\equiv\text{C—H} + \text{Ph—NH}_2 \longrightarrow \text{Ph—CH=CH—N(Ph)—Ph}$					
Entry	Catalyst	Co-catalyst ^b	t (h)	Conv. (%)	Selec. (%)
1	$\text{KPhos}(\text{AuNTf}_2)$	—	2	85	98
2	$\text{KPhos}(\text{AuCl})$	AgBF_4	23	100	98
3	$\text{KPhos}(\text{AuCl})$	AgOTf	2	100	94
4	$\text{KPhos}(\text{AuCl})$	AgNTf_2	2	100	100
5	$\text{KPhos}(\text{AuCl})$	$\text{CH}_3\text{CN}/\text{NH}_4\text{BF}_4$	1.5	100	97
6	$\text{KPhos}(\text{AuCl})$	—	27	53	53
7	AgBF_4	—	24	28	45

^a Reaction conditions: T : 70 °C, amine (0.17 mmol), alkyne (0.15 mmol), toluene (0.5 mL) and cat. (3.3 mg, 3.2 μmol , 2 mol% based on Au).

^b Co-catalyst: 2.2 mol%.



Experimental

Materials

$\text{RuHClCO}(\text{PPh}_3)_3$ and $\text{AuX}(\text{PPh}_3)$ ($\text{X} = \text{Cl}, \text{NTf}_2$) complexes were prepared according to the literature.³¹ Triphenylphosphine, biphenyl, iron trichloride, aluminium trichloride, ruthenium trichloride, chloro(tetrahydrothiophene)gold(i) and potassium tetrachloroaurate(III) were obtained from commercial sources.

Preparation of polymers

Synthesis of KPhos(Ru). In a sealed tube, using a procedure similar to that previously reported for knitted polymers,¹⁰ $[\text{RuHClCO}(\text{PPh}_3)_3]$ (118 mg, 0.134 mmol) in dichloromethane (10 mL) was flushed with N_2 . After 15 minutes, AlCl_3 (1.58 g, 12.03 mmol) was added and the mixture heated at 40 °C for 72 hours. Then, the solid was washed with dichloromethane, HCl (aq) 4% (vol), tetrahydrofuran and acetone and the brown resulting solid dried at 70 °C overnight. Yield 90%. Elemental analysis found: % C 47.9, % H 3.9. TXRF analysis: % Ru 22.0, % P 14.1.

Synthesis of KPhos(Ru)Bi. Following the above method, biphenyl (32.4 mg, 0.210 mmol) was added to a solution of $[\text{RuHClCO}(\text{PPh}_3)_3]$ (100 mg, 0.105 mmol) in dichloromethane (12 mL). After flushing with N_2 for 15 minutes, AlCl_3 (1.40 g, 10.5 mmol) was added and the mixture heated at 40 °C for 72 hours. The same work-up was employed. Yield: 97%. Elemental analysis found: % C 64.3, % H 4.12. TXRF analysis: % Ru 8.0, % P 4.9.

Synthesis of KPhos(AuCl). Following the above method, $(\text{PPh}_3)\text{AuCl}(\text{PPh}_3)$ (401.4 mg, 0.813 mmol) and AlCl_3 (1.08 g, 8.13 mmol) were refluxed in dichloromethane (63 mL) for 48 h. The same work-up was employed. Yield 96%. Elemental analysis found: % C 42.5, % H 3.37. ICP analysis: % Au 19.0, % P 15.0.

Synthesis of KPhos(AuNTf₂). Following the above method $(\text{PPh}_3)\text{Au}(\text{NTf}_2)$ (500 mg, 0.676 mmol) and AlCl_3 (0.90 g, 6.76 mmol) were heated at 40 °C in dichloromethane (65 mL) for 48 h. Yield 98%. The same work-up was employed. Elemental analysis found: % C 82.2, % H 5.56. ICP analysis: % Au 14.9, % P 13.3.

Synthesis of KPhosBi. Triphenylphosphine (2.63 g, 0.01 mol) and biphenyl (1.54 g, 0.01 mol) were dissolved in dichloroethane (20 mL). After purging with N_2 for 15 minutes, dimethoxymethane (2.65 mL, 0.06 mol) and AlCl_3 (4.0 g, 0.06 mol) were added and the mixture was heated at 80 °C for 48 hours. The same washing protocol as for KPhosRu was employed. Elemental analysis found: % C 82.2, % H 5.56. TXRF analysis: % P 1.5.

Post-functionalization with RuCl_3 (KPhosBi(Ru)). The previously formed polymer KPhosBi (1.52 g) was heated at reflux in formaldehyde and 2-methoxyethanol (1:4) with $\text{RuCl}_3 \cdot n\text{H}_2\text{O}$ (160 mg, 0.77 mmol)³² for 48 h. The resulting polymer was washed twice with each solvent in the following order: methanol, water, acetone and tetrahydrofuran. Elemental analysis found: % C 85.4, % H 5.66. TXRF analysis: % Ru 0.02, % P 1.5.

Post-functionalization with $\text{AuCl}(\text{tht})$ (KPhosBi(Au)). KPhosBi (100 mg) was heated under reflux in ethanol (20 mL) with $\text{AuCl}(\text{tht})$ (107 mg, 0.530 mmol)³² overnight. The resulting solid was washed with dichloromethane, methanol, acetone and tetrahydrofuran. Elemental analysis found: % C 52.9, % H 3.44. TXRF analysis: % Au 2.0, % P 1.5.

Catalytic activity

Typical procedure for the synthesis of imines. In a 5 mL SUPELCO reactor: 0.1 mmol of amine, 0.12 mmol of benzyl alcohol and 2.0 mg of KPhosRu in 0.5 mL of toluene were mixed and heated at 100 °C for the corresponding time (Table 2). The conversion was analyzed by GC-MS chromatography.

Typical procedure for the hydration of alkynes. a) without co-catalyst: alkyne (0.2 mmol), 10 mg (7.2 μmol) of KPhos(AuNTf₂), 0.4 mL of methanol and 20 μL of H_2O were introduced into a 5 mL SUPELCO reactor and the mixture heated under stirring at 60 °C for the corresponding time (Table 4); b) in the presence of co-catalyst: in a 5 mL SUPELCO reactor: alkyne (0.2 mmol), KPhos(AuCl) (10 mg, 9.7 μmol) and co-catalyst (10.7 μmol) were mixed in 0.4 mL of methanol and 20 μL of H_2O at 60 °C for the corresponding time (Table 3).

Typical procedure for the hydroamination of alkynes. In a 5 mL SUPELCO reactor: aniline (0.17 mmol), alkyne (0.15 mmol), KPhos(AuX) (3.3 mg, 3.2 μmol) and co-catalyst (3.52 μmol) were mixed in dry toluene (0.5 mL) at 70 °C. Conversion was analysed by GC-MS (Table 5).

Some representative examples of the chromatograms obtained are recorded in Fig. S21–S25.†

Conflicts of interest

There are no conflicts to declare.

Acknowledgements

The authors acknowledge MINEICO of Spain MAT2017-82288-C2-2-P project for financial support. AVG thanks Ministerio de Educación y Formación Profesional for FPU17/03463.

Notes and references

- (a) Z. Wang, G. Chen and K. Ding, Self-Supported Catalysts, *Chem. Rev.*, 2009, **109**, 322–359; (b) Z. Wang, G. Chen and K. Ding, *Chem. Rev.*, 2008, **109**, 322–359; (c) P. Barbaro and F. Liguori, *Heterogenized homogeneous catalysts for fine chemicals production: materials and processes*, Springer Science & Business Media, 2010, vol. 33.
- (a) H. Zhou, Y. M. Wang, W. Z. Zhang, J. P. Qu and X. B. Lu, *Green Chem.*, 2011, **13**, 644–650; (b) H. Q. Yang, G. Li, Z. C. Ma, J. B. Chao and Z. Q. Guo, *J. Catal.*, 2010, **276**, 123–133.
- (a) H. Yang, Y. Wang, Y. Qin, Y. Chong, Q. Yang, G. Li, L. Zhang and W. Li, *Green Chem.*, 2011, **13**, 1352; (b) K. V. S. Ranganath, J. Kloesges, A. H. Schäfer and F. Glorius, *Angew. Chem., Int. Ed.*, 2010, **49**, 7786–7789.
- M. Gruttadauria, F. Giacalone and R. Noto, *Chem. Soc. Rev.*, 2008, **37**, 1666–1688.



- 5 (a) M. Pintado-Sierra, A. M. Rasero-Almansa, A. Corma, M. Iglesias and F. Sánchez, *J. Catal.*, 2013, **299**, 137–145; (b) A. M. Rasero-Almansa, A. Corma, M. Iglesias and F. Sánchez, *Green Chem.*, 2014, **16**, 3522–3527; (c) F. J. Song, C. Wang, J. M. Falkowski, L. Q. Ma and W. B. Lin, *J. Am. Chem. Soc.*, 2010, **132**, 15390–15398.
- 6 (a) P. Kaur, J. T. Hupp and S. T. Nguyen, *ACS Catal.*, 2011, **1**, 819–835; (b) A. Trewin and A. I. Cooper, *Angew. Chem., Int. Ed.*, 2010, **49**, 1533–1535; (c) W. Wang, A. Zheng, P. Zhao, Ch. Xia and F. Li, *ACS Catal.*, 2014, **4**, 321–327; (d) D. Wu, F. Xu, B. Sun, R. Fu, H. He and K. Matyjaszewski, *Chem. Rev.*, 2012, **112**, 3959–4015; (e) Y. Zhang and S. N. Riduan, *Chem. Soc. Rev.*, 2012, **41**, 2083–2094; (f) L. Tan and B. Tan, *Chem. Soc. Rev.*, 2017, **46**, 3322–3356.
- 7 S. Y. Ding and W. Wang, *Chem. Soc. Rev.*, 2013, **42**, 548–568.
- 8 (a) R. K. Totten, M. H. Weston, J. K. Park, O. K. Farha, J. T. Hupp and S. T. Nguyen, *ACS Catal.*, 2013, **3**, 1454–1459; (b) A. M. Shultz, O. K. Farha, J. T. Hupp and S. T. Nguyen, *Chem. Sci.*, 2011, **2**, 686–689; (c) K. K. Tanabe, N. A. Siladke, E. M. Broderick, T. Kobayashi, J. F. Goldston, M. H. Weston, O. K. Farha, J. T. Hupp, M. Pruski, E. A. Mader, M. J. A. Johnson and S. T. Nguyen, *Chem. Sci.*, 2013, **4**, 2483–2489.
- 9 (a) B. Li, R. Gong, W. Wang, X. Huang, W. Zhang, H. Li, C. Hu and B. Tan, *Macromolecules*, 2011, **44**, 2410–2414; (b) R. T. Woodward, L. A. Stevens, R. Dawson, M. Vijayaraghavan, T. Hasell, I. P. Silverwood, A. V. Ewing, T. Ratvijitvech, J. D. Exley, S. Y. Chong, F. Blanc, D. J. Adams, S. G. Kazarian, C. E. Snape, T. C. Drage and A. I. Cooper, *J. Am. Chem. Soc.*, 2014, **136**, 9028–9035; (c) L. Li, K. Cai, P. Wang, H. Ren and G. Zhu, *ACS Appl. Mater. Interfaces*, 2015, **7**, 201–208; (d) L. Li, H. Ren, Y. Yuan, G. Yu and G. Zhu, *J. Mater. Chem. A*, 2014, **2**, 11091–11098.
- 10 (a) K. J. Msayib and N. B. McKeown, *J. Mater. Chem. A*, 2016, **4**, 10110–10113; (b) S. Wang, Ch. Zhang, Y. Shu, S. Jiang, Q. Xia, L. Chen, S. Jin, I. Hussain, A. I. Cooper and B. Tan, *Sci. Adv.*, 2017, **3**, e1602610; (c) E. M. Maya, E. Rangel-Rangel, U. Díaz and M. Iglesias, *J. CO₂ Util.*, 2018, **25**, 170–179; (d) J. Guadalupe, A. M. Ray, E. M. Maya, B. Gómez-Lor and M. Iglesias, *Polym. Chem.*, 2018, **9**, 4585–4595.
- 11 X. Wang, S. Min, S. K. Das, W. Fan, K. Huang and Z. Lai, *J. Catal.*, 2017, **355**, 101–109.
- 12 Ch. Tang, Z. Zou, Y. Fu and K. Song, *ChemistrySelect*, 2018, **3**, 5987–5992.
- 13 X. Wang, E. A. P. Ling, Ch. Guan, Q. Zhang, W. Wu, P. Liu, N. Zheng, D. Zhang, S. Lopatin, Z. Lai and K.-W. Huang, *ChemSusChem*, 2018, **11**, 3591–3598.
- 14 TXRF technique did not allow the quantification of gold since K phosphorous lines and M gold lines are overlapped.
- 15 (a) H. Li, F. Zhang, Y. Wan and Y. Lu, *J. Phys. Chem. B*, 2006, **110**, 22942; (b) W. He, F. Zhang and H. Li, *Chem. Sci.*, 2011, **2**, 961–966.
- 16 (a) B. Li, Z. Guan, W. Wang, X. Yang, J. Hu, B. Tan and T. Li, *Adv. Mater.*, 2012, **24**, 3390–3395; (b) C. Wang, Y. Han, Y. Li, K. Nie, X. Cheng and J. Zhang, *RSC Adv.*, 2016, **6**, 34866–34871.
- 17 (a) D. S. Glueck, *Organophosphorus Chemistry: From Molecules to Applications*, ed. V. Laroshenko, Wiley-VCH, 2019, p. 457; (b) A. C. Vetter, K. Nikitin and D. G. Gilheany Phosphorus, Sulfur, and Silicon and the Related Elements, 2019, DOI: 10.1080/10426507.2018.1541242.
- 18 D. J. Morgan, *Surf. Interface Anal.*, 2015, **47**, 1072–1079.
- 19 (a) Triphenylphosphine stability: K. Moedritzer and R. E. Miller, *J. Therm. Anal.*, 1969, **1**, 151–157. For gold oxides stability: (b) O. Díaz-Morales, F. Calle-Vallejo, C. de Munck and M. T. M. Koper, *Chem. Sci.*, 2013, **4**, 2334–2343; (c) A. Kawamoto, H. Ando, H. Ohashi, Y. Kobayashi, T. Honma, T. Ishida, M. Tokunaga, Y. Okaue, S. Utsunomiya and T. Yokoyama, *Bull. Chem. Soc. Jpn.*, 2016, **11**, 1385–1390. For ruthenium oxides stability: (d) J. S. Punni and P. K. Mason, *AEAT-1277 Report*, Harwell, 1998.
- 20 (a) Z. Jia, K. Wang, B. Tan and Y. Gu, *Adv. Synth. Catal.*, 2017, **359**, 78–88; (b) Q. Wang, L. Zhang, L. Hao, Ch. Wang, Q. Wu and Z. Wang, *J. Chromatogr. A*, 2018, **1575**, 18–25.
- 21 (a) A. J. A. Watson and J. M. J. Williams, *Science*, 2010, **329**, 635–636; (b) C. Gunanathan and D. Milstein, *Science*, 2013, **341**, 249–260.
- 22 (a) J. P. Adams, *Perkin 1*, 2000, **1**, 125–139; (b) J. Gawronski, N. Wascinska and J. Gajewy, *Chem. Rev.*, 2008, **108**, 5227–5252.
- 23 B. Chen, J. Li, W. Dai, L. Wanga and S. Gao, *Green Chem.*, 2014, **16**, 3328–3334.
- 24 (a) A. Corma, J. Navas and M. J. Sabater, *Chem. Rev.*, 2018, **118**, 1410–1459; (b) K. Sordakis, C. Tang, L. K. Vogt, H. Junge, P. J. Dyson, M. Beller and G. Laurenczy, *Chem. Rev.*, 2018, **118**, 372–433.
- 25 (a) B. hen, L. Wang and S. Gao, *ACS Catal.*, 2015, **5**, 5851–5876; (b) M. Mon, R. Adam, J. Ferrando-Soria, A. Corma, D. Armentano, E. Pardo and A. Leyva-Pérez, *ACS Catal.*, 2018, **8**, 10401–10406.
- 26 W. Kuriyama, *Encyclopedia of Reagents for Organic Synthesis*, 2014, vol. 1, DOI: 10.1002/047084289X.rm01699.
- 27 (a) A. Corma, J. Navas and M. J. Sabater, *Chem. Rev.*, 2018, **118**, 1410–1459; (b) H. Wu, J. Wu and Z. Du, *Chin. J. Org. Chem.*, 2017, **37**, 1127–1138; (c) B. Gnanaprakasam, E. Balaraman, Y. Ben-David and D. Milstein, *Angew. Chem., Int. Ed.*, 2011, **50**, 12240–12244; (d) P. Hu, Y. Ben-David and D. Milstein, *Angew. Chem., Int. Ed.*, 2016, **55**, 1061–1064.
- 28 D. Wang, R. Cai, S. Sharma, J. Jirak, S. K. Thummanapelli, N. G. Akhmedov, H. Zhang, X. Liu, J. L. Petersen and X. Shi, *J. Am. Chem. Soc.*, 2012, **134**, 9012–9019.
- 29 A. Leyva and A. Corma, *J. Org. Chem.*, 2009, **5**, 2067–2074.
- 30 L. Huang, M. Arndt, K. Gooßen, H. Heydt and L. J. Gooßen, *Chem. Rev.*, 2015, **115**, 2596–2697.
- 31 (a) Synthesis of Ru-complex: A. López, A. Romero, A. Santos, A. Vegas, A. M. Echavarren and P. Noheda, *J. Organomet. Chem.*, 1989, **373**, 249–258. Synthesis of (Ph₃P)AuCl; (b) M. I. Bruce, B. K. Nicholson and O. Bin Shawkataly, *Inorg. Synth.*, 1989, **26**, 324–328. Synthesis of (Ph₃P)Au(NTf₂); (c) N. Mezailles, L. Ricard and F. Gagosz, *Org. Lett.*, 2005, **7**, 4133–4136.
- 32 The metal amount was based on the phosphorous loading of the polymer being 0.5% in polymer weight, 1.6×10^{-4} mmol g⁻¹ of polymer.

